ELECTROWEAK RESULTS FROM THE TEVATRON

Darien Wood*
Fermi National Accelerator Laboratory
Batavia, Illinois 60510

Representing the CDF and DØ Collaborations

ABSTRACT

Electroweak results are presented from the CDF and DØ experiments based on data collected in recent runs of the Fermilab Tevatron Collider. The measurements include the mass and width of the W boson, the production cross sections of the W and Z bosons, and the W charge asymmetry. Additional results come from studies of events with pairs of electroweak gauge bosons and include limits on anomalous couplings.

*Present address: Department of Physics, Northeastern University, Boston, MA 02115.

1 Introduction

In high-energy $\bar{p}p$ collisions, it is possible to study electroweak physics by direct observation of the carriers of the weak force, W and Z bosons. W bosons, in particular, have been produced and detected only at the CERN S$\bar{p}p$S (closed since 1991) and at the Fermilab Tevatron Collider. The large samples of W bosons produced in hadron colliders complement the detailed studies of the Z boson at the e^+e^- colliders, LEP and SLC.

It is interesting to track the number of W bosons detected by experiments over the years, as shown in Fig. 1. From the handful of events that established the existence of W and Z bosons at CERN in 1982 (Refs. 1 and 2), the samples available now to the Tevatron experiments number in the tens of thousands. This steady increase in statistics has yielded corresponding increases in the precision of electroweak measurements and in the variety of electroweak properties that are studied at the hadron collider experiments.

Almost all results presented here come from the recent runs of the Tevatron Collider and from its two collider experiments: CDF (Ref. 3) and DØ (Ref. 4). The run which took place in 1992–93 is referred to as "Run 1A," and it resulted in integrated luminosities of about 13–20 pb^{-1} per experiment. The run which began in early 1994 and which is still in progress is called "Run 1B" and is expected to yield ≈ 100 pb^{-1}. In both runs, the $\bar{p}p$ collisions have a center-of-mass energy of $\sqrt{s} = 1.8$ TeV. Final results are available for most of the Run 1A analyses, and some preliminary results based on part of the Run 1B data are included as well.

Since their hadronic decay modes are difficult to distinguish from the large background from QCD multijet production, these gauge bosons are usually studied through their leptonic decay modes: $W \to \ell\nu$ and $Z \to \ell^+\ell^-$.

2 W and Z Boson Production Studies

At lowest order, W and Z bosons are produced via quark-antiquark annihilation. Higher order contributions, which can include gluons in the initial and final states, increase the total cross section and create a nonzero transverse momentum spectrum for the W and Z bosons. Thus, the total production rate of W and Z bosons depends on many factors outside the scope of pure electroweak theory, especially parton distribution functions and QCD corrections. Some electroweak properties

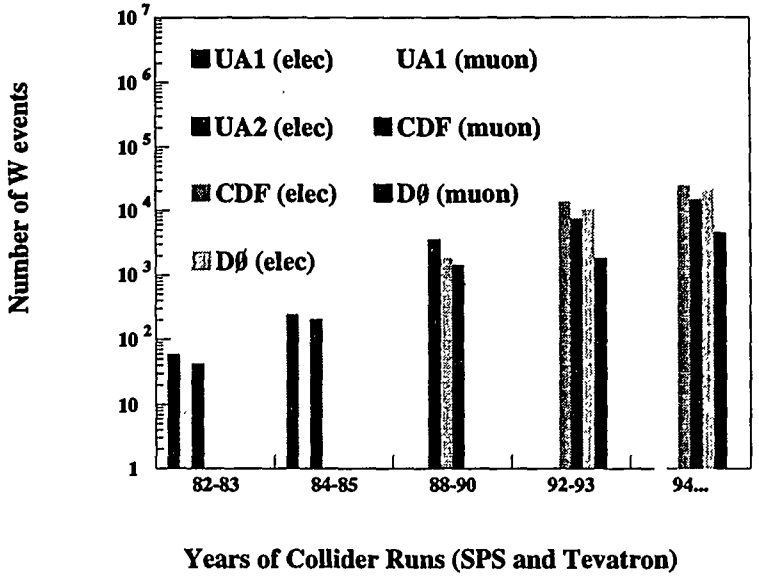

Figure 1: Number of W boson events observed by experiments as a function of the years of hadron collider runs.

can be revealed, however, by examining production rates as a function of boson type and lepton charge and rapidity.

2.1 Production Cross Sections and Indirect Γ_W Measurement

The details of selection of events vary slightly among the different analyses, but, in general, are quite similar. For W bosons, a high-p_T isolated lepton ($p_T^\ell > 20$–25 GeV) is required along with missing transverse energy ($\not\!\!E_T > 20$–25 GeV) which is identified as the neutrino transverse momentum (p_T^ν). The Z event selection generally requires two high-p_T ($p_T^\ell > 15$–25 GeV) leptons and an invariant mass for the pair near the Z boson mass. The principal backgrounds are QCD multijet events with fake leptons and/or $\not\!\!E_T$, decays $W \to \tau\nu, \tau \to \ell\nu\bar{\nu}$, and (in the muon channel only) cosmic rays. Figure 2 shows an example[5] of the W transverse mass ($M_T = \sqrt{(p_T^\ell + p_T^\nu)^2 - (\vec{p}_T^{\,\ell} + \vec{p}_T^{\,\nu})^2}$) and Z invariant mass distributions after selection cuts.

The rate of W and Z bosons observed by the experiments is proportional to the product of production cross section and leptonic branching fraction. The measurements of this product in the electron and muon channels are given in Table 1 (Refs. 5–7). Also shown is the ratio of $\sigma \cdot B$ for W and Z production:

$$R_\ell = \frac{\sigma(\bar{p}p \to W \to \ell\nu)}{\sigma(\bar{p}p \to Z \to \ell\ell)} = \frac{\sigma(\bar{p}p \to W)}{\sigma(\bar{p}p \to Z)} \cdot \frac{\Gamma(W \to \ell\nu)}{B(Z \to \ell\ell)} \cdot \frac{1}{\Gamma_W}. \qquad (1)$$

R_ℓ is predicted more precisely than the individual cross sections because many of the QCD and parton-distribution effects partially cancel. Experimentally, it has the advantage that the luminosity errors cancel completely and the efficiency errors cancel partially. The world R_ℓ measurements[5–9] (excluding preliminary results) and their averages are shown in Fig. 3. The ratio of production cross sections predicted at $O(\alpha_s^2)$ (Ref. 10) is 3.33 ± 0.03 (3.26 ± 0.09) at $\sqrt{s} = 1.8$ TeV (0.63 TeV). The branching ratio $B(Z \to \ell\ell) = (3.367 \pm 0.006)\%$ can be taken from the LEP experiments.[11] With these inputs, Eq. (1) can be used to transform the R_ℓ measurement into a determination of the W leptonic branching ratio: $B(W \to \ell\nu) = (10.9 \pm 0.3)\%$. If, in addition, we assume the Standard Model prediction for the partial decay width $\Gamma(W \to \ell\nu) = 225.2 \pm 1.5$ MeV (Ref. 12), then we obtain an indirect measurement of the total width of the W boson: $\Gamma_W = 2.062 \pm 0.059$ GeV. This can be compared with the Standard Model prediction

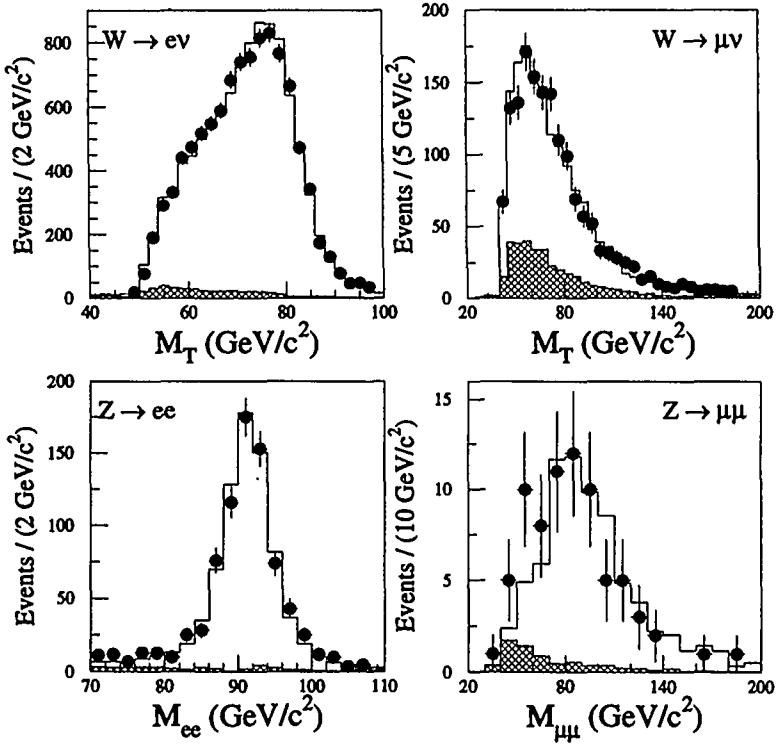

Figure 2: W transverse mass distributions and Z invariant mass distributions from the DØ Run 1A cross-section analysis.

	$\sigma \cdot B(W \to \ell\nu)$ (nb)	$\sigma \cdot B(Z \to \ell\ell)$ (nb)	R_ℓ
1988/'89 data			
CDF(e)	$2.19 \pm 0.04 \pm 0.21$	$0.209 \pm 0.013 \pm 0.017$	$10.2 \pm 0.8 \pm 0.4$
CDF(μ)	2.21 ± 0.22	0.226 ± 0.032	9.8 ± 1.2
Run 1A			
CDF(e)	2.49 ± 0.12	0.231 ± 0.012	$10.90 \pm 0.32 \pm 0.29$
DØ(e)	$2.36 \pm 0.02 \pm 0.15$	$0.218 \pm 0.008 \pm 0.014$	$10.82 \pm 0.41 \pm 0.30$
DØ(μ)	$2.09 \pm 0.06 \pm 0.25$	$0.178 \pm 0.022 \pm 0.023$	$11.8 \pm 1.6 \pm 1.1$
Run 1B			
(prelim.)			
DØ(e)	$2.24 \pm 0.02 \pm 0.20$	$0.226 \pm 0.006 \pm 0.021$	$9.9 \pm 0.3 \pm 0.8$
DØ(μ)	$1.93 \pm 0.04 \pm 0.20$	$0.159 \pm 0.014 \pm 0.022$	$12.3 \pm 1.1 \pm 1.2$

Table 1

of $\Gamma_W = 2.077 \pm 0.014$ GeV (Ref. 12). This comparison results in an upper limit (95% CL) of 109 MeV for the excess decay width of the W boson which can be used to put limits on any new final states into which the W might decay.

2.2 Direct Γ_W Measurement

The CDF experiment also estimates the W total width with a direct fit[13] of the transverse mass spectrum of $W \to e\nu$ events, shown in Fig. 4. The high transverse mass region of the distribution is sensitive to the width of the Breit-Wigner line shape. A fit to the transverse mass above 110 GeV results in a determination $\Gamma_W = 2.11 \pm 0.28 \pm 0.16$ GeV. Although the uncertainties are larger than those from the indirect ratio method, this direct width determination requires fewer Standard Model assumptions.

2.3 W Charge Asymmetry

The measurement of the lepton charge asymmetry in W boson events gives additional information about the production properties. The different momentum distributions of *up* and *down* quarks in the proton give rise to an asymmetry in the production of W bosons: a W^+ is more likely to follow the direction of the

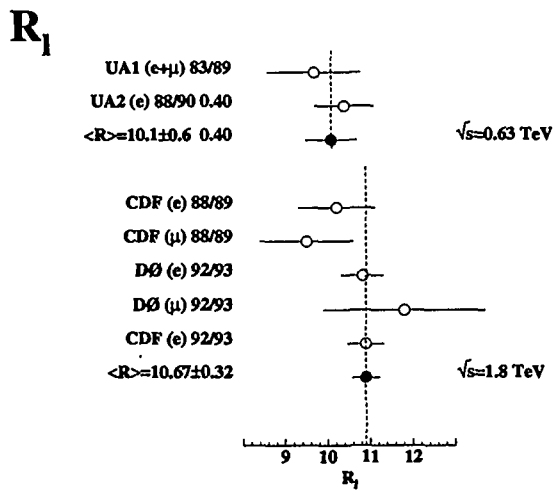

Figure 3: World measurements of R_ℓ, the ratio of W to Z cross sections times leptonic branching ratio.

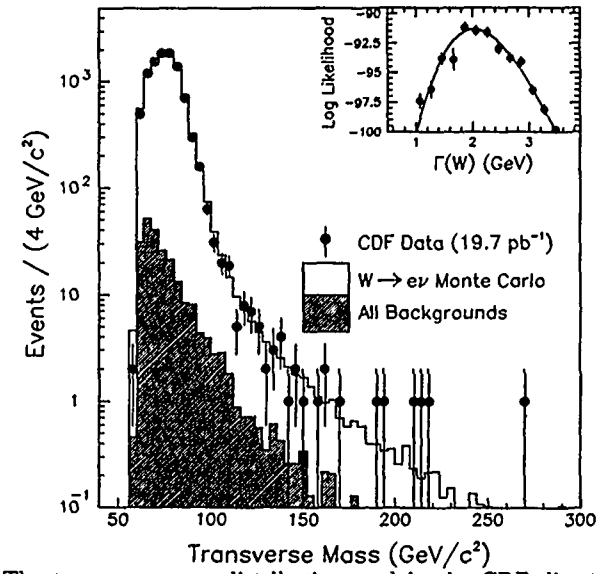

Figure 4: The transverse mass distribution used in the CDF direct fit of the W boson width. The fit is made in the region $M_T > 110$ GeV.

proton beam. When the boson decays, this is also asymmetric due to the $V-A$ couplings, and the tendency is opposite, sending the ℓ^+ back toward the antiproton direction in the W boson rest frame. In the lab frame, one sees the combined effect in the charge asymmetry of leptons from W boson decays as a function of pseudorapidity (η), with the production asymmetry dominating in most cases. For W boson production at $\sqrt{s} = 1.8$ TeV, the asymmetry is especially sensitive to the slope of $u(x)/d(x)$ for $0.007 < x < 0.27$, where x is the fraction of proton momentum carried by the interacting quark or antiquark.

The lepton charge asymmetry is defined as $A(\eta) = (N_{\ell^+}(\eta) - N_{\ell^-}(\eta))/(N_{\ell^+}(\eta) + N_{\ell^-}(\eta))$. The CDF measurement[14] of $A(\eta)$ from Run 1A has been published and has been used to constrain the parton distribution functions (pdf's). This is important, for example, in the W mass measurement, where pdf uncertainties can contribute significantly to the uncertainty in the final result. Figure 5 shows preliminary asymmetry distributions from Run 1A and part of Run 1B combined. The CDF points are from about 67 pb^{-1} from both electrons and muons, and the DØ points are from about 36 pb^{-1} from muons only. The curves show the NLO Monte Carlo predictions[15] using several pdf sets.[16-18] The older sets which were disfavored by the CDF Run 1A asymmetry[14] are not shown in the figure. The pdf sets shown have included the CDF Run 1A asymmetry as part of their input data, and all three sets are in good agreement with the new data.[19]

3 W Boson Mass

The W mass measurement is the most precise electroweak measurement from the hadron colliders. The favored technique involves fitting the M_T spectra of the W bosons to simulated spectra generated with different W masses. The p_T spectra of the charged lepton and of the neutrino also carry information about the mass, but they are more sensitive to the transverse momentum distribution of the W boson itself than is M_T.

The CDF measurement from Run 1A (Ref. 20) described here is now finalized. Figure 6 shows the M_T distributions which are fit. The electron and muon channels are fit separately, with the results $M_W(\mu) = 80.310 \pm 0.205 \pm 0.130$ GeV, $M_W(e) = 80.490 \pm 0.145 \pm 0.175$ GeV, where the first error is statistical and the second is systematic. The combined result is $M_W = 80.410 \pm 0.180$. The contributions to the uncertainties are summarized in Table 2.

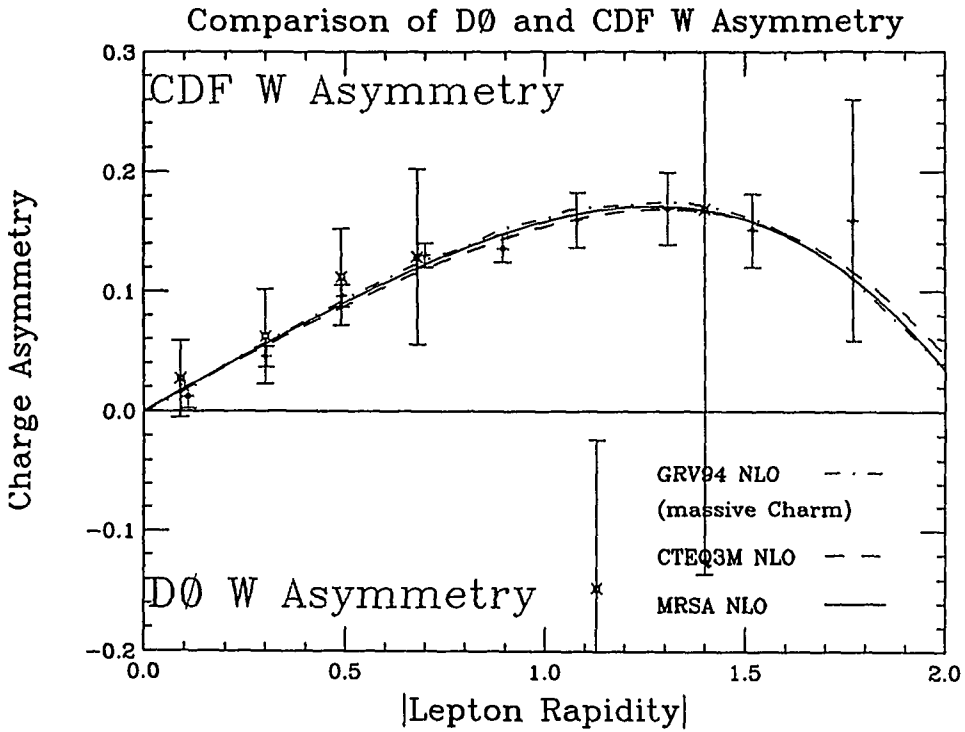

Figure 5: Preliminary lepton charge asymmetries from the W boson samples from Run 1A plus part of Run 1B. The crosses are from CDF, electrons and muons (67 pb^{-1}), and the x's from DØ, muons only (36 pb^{-1}).

Source	e	μ	Common
Statistical	145	205	–
Energy scale	120	50	50
E or p resolution	80	60	–
p_T^W and recoil model	75	75	65
pdf's	50	50	50
QCD/QED corrections	30	30	30
W width	20	20	20
Backgrounds/bias	30	40	5
Fitting procedure	10	10	–
Total	230	240	100
Combined	180		

Table 2: Uncertainties on M_W (MeV) for CDF Run 1A.

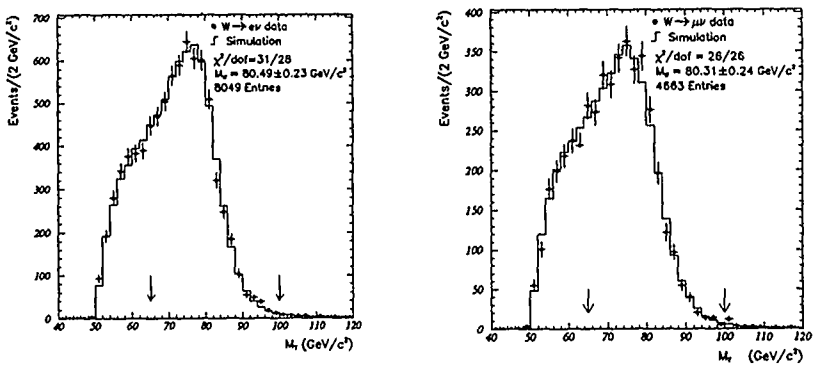

Figure 6: The CDF mass fits to the W boson transverse mass spectra from Run 1A. The electron channel is shown on the left and the muon channel on the right.

The energy scale for the leptons is calibrated first for muons. A sample of about 60,000 $J/\psi \to \mu\mu$ events is used to set the momentum scale in the CDF spectrometer. The ratio between the fit to $\mu\mu$ invariant mass spectrum is shown in Fig. 7 and the world average for the J/ψ mass yields a momentum correction factor 0.999984 ± 0.00058. The error includes the contribution from the uncertainty in the extrapolation from the transverse momenta for the muons from J/ψ decay (typically $\sim$ 3 GeV) to those from W boson decays (typically $\sim$ 40 GeV). This calibration uncertainty results in a contribution of 50 MeV to the W mass uncertainty in the muon channel. After this correction, the scale is checked with the peaks for $\Upsilon \to \mu\mu$ (shown in Fig. 8) and $Z \to \mu\mu$.

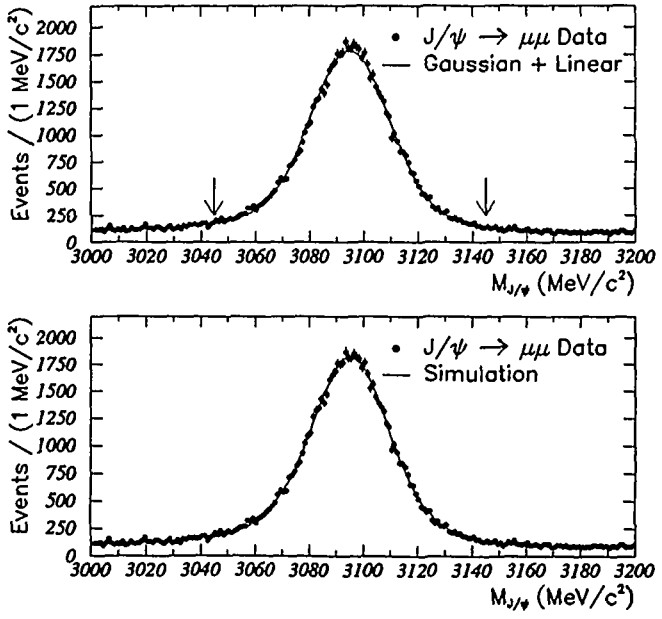

Figure 7: The $J/\psi \to \mu\mu$ invariant mass spectra used in determining the momentum scale used in the CDF W boson mass measurement. A simple fit (top) and the result of the Monte Carlo simulation (below) are compared to the data.

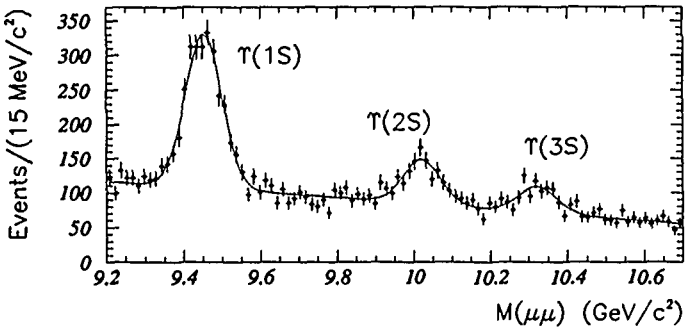

Figure 8: Comparison of measured and predicted upsilon resonance peaks are used to check the momentum calibration of the CDF spectrometer.

The electron transverse energies are determined from their measurement in the calorimeter. In order to set the calibration of the electromagnetic calorimeter, the momentum from the spectrometer is compared to the energy measured in the calorimeter for a sample of electrons from W decays. The scale of the calorimeter is adjusted until the measured E/p ratio (shown in Fig. 9) agrees with that expected. This transfer procedure contributes 110 MeV to the calibration uncertainty on M_W, yielding a total calibration uncertainty of 120 MeV in the electron channel.

Recall that M_T depends on $\vec{p}_T^{\,\ell}$ and $\vec{p}_T^{\,\nu}$. Since $\vec{p}_T^{\,\nu}$ is determined from the missing $\vec{p}_T$, it depends on $\vec{u}$, the measured transverse momentum of the hadrons recoiling against the W direction: $\vec{p}_T^{\,\nu} = \vec{p}_T = \vec{p}_T^{\,W} - \vec{p}_T^{\,\ell} = -\vec{u} - \vec{p}_T^{\,\ell}$. Many systematic studies, therefore, concentrate on properly modeling the measurement of $\vec{p}_T^{\,\ell}$ and $\vec{u}$. Once the lepton scale is established, the uncertainties from the p_T^W distribution and from the measurement of u must be established. In most cases, this is done using the $Z \to \ell\ell$ events, where each event has independent measurements of p_T^W from the hadrons and from the leptons. Underlying events from real Z events are used directly in the W simulation to model the recoil response of the detector. The distribution that is used to control this process is $u_\perp$, the component of $\vec{u}$ perpendicular to the lepton direction in $W \to \ell\nu$ events. The p_T distribution of the Z events used in the W simulation is scaled until the $u_\perp$ distribution of the simulation matches that of the W sample events, as shown in Fig. 10. The

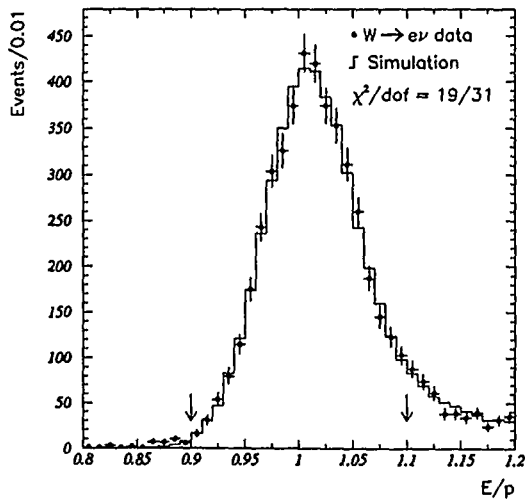

Figure 9: The CDF ratio of energy measured in the calorimeter to momentum measured in the spectrometer for the $W \rightarrow e\nu$ sample. This distribution is used in the transfer of the energy calibration scale to the calorimeter.

uncertainty in M_W resulting from the remaining uncertainty on p_T^W is 45 MeV. In addition, there is a 60 MeV uncertainty due to the modeling of the recoil measurement.

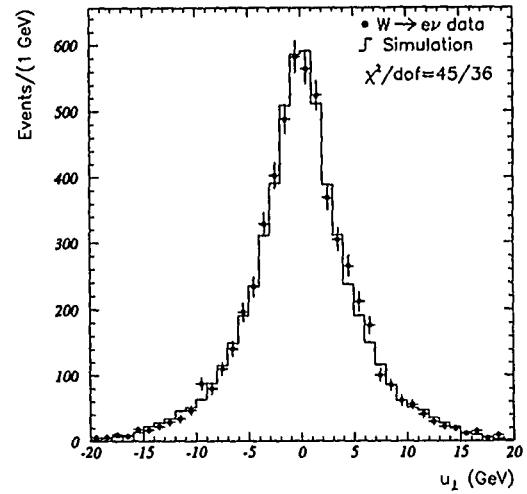

Figure 10: The CDF distribution of $u_\perp$ (see text) in $W \rightarrow e\nu$ events (points), compared with the simulation model (histogram).

The pdf's largely determine the longitudinal production distribution of the W bosons and consequently influence the observed transverse mass distribution after acceptance effects are taken into account. The best constraints on the pdf uncertainties come from the measurement of the W charge asymmetry described earlier. Figure 11 shows the change in the measured mass for different pdf sets, with respect to that obtained with the MRS D'_ pdf set. The abscissa in this figure is a measure of the deviation of the CDF Run 1A measured charge asymmetry from that predicted by each pdf set, and the uncertainty on M_W is obtained by considering only those sets which are within $\pm 2\sigma$ from the best agreement with the asymmetry. The uncertainty from pdf's is thus determined to be 50 MeV.

The M_W results just described are shown in Fig. 12 along with other currently available measurements of the W (Refs. 21–23). The DØ measurement[23]

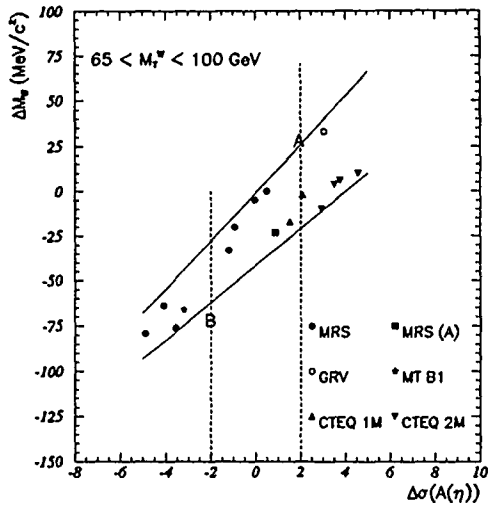

Figure 11: The change in the fitted W boson mass is plotted against the deviation from the CDF Run 1A data of the predicted asymmetry for various pdf's. The lines show the limits used in establishing the uncertainty on M_W.

is preliminary and is expected to be superseded by a final result soon. A preliminary world average of 80.26 ± 0.16 GeV is also shown, which was obtained assuming a common systematic error of 85 MeV among the different measurements. The precision electroweak measurements of the Z boson from LEP[24] and SLC[25] are also sensitive to the W mass through the relationship between M_W and $sin^2\theta_W$, and the corresponding predictions for M_W are shown as well. The hadron collider measurement is in very good agreement with the LEP prediction but disagrees somewhat with the SLC prediction. Another indirect measurement of $M_W = 80.24 \pm 0.25$ GeV is obtained from the $sin^2\theta_W$ measurement in neutrino scattering,[26] which is also in good agreement with the direct measurement.

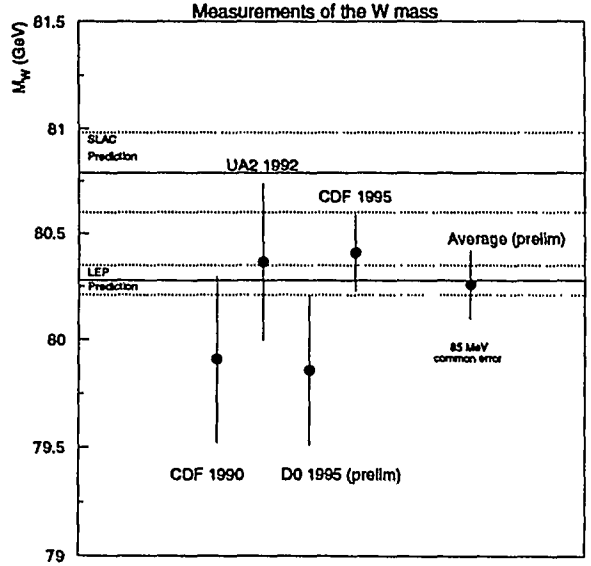

Figure 12: The direct measurements of M_W from hadron collider experiments and their average (points) is compared to predictions based on Z pole measurements at LEP and SLC (horizontal bands).

In the Standard Model, the value of M_W is sensitive to the mass of the top quark (quadratically) and to the mass of the Higgs boson (logarithmically) through radiative corrections. This relationship is shown in Fig. 13 for three different values of the Higgs mass.[27] The uncertainties on the predictions are shown as the dotted

lines and are dominated by uncertainties on the value of α_{EM} at the vector boson masses. The world average for M_W is plotted along with the average value of the top quark mass from CDF (Ref. 28) and DØ (Ref. 29). With the present uncertainties, the data are consistent with all the values of the Higgs mass shown, but more precise future measurements of M_W and M_{top} might be able to constrain M_{Higgs}.

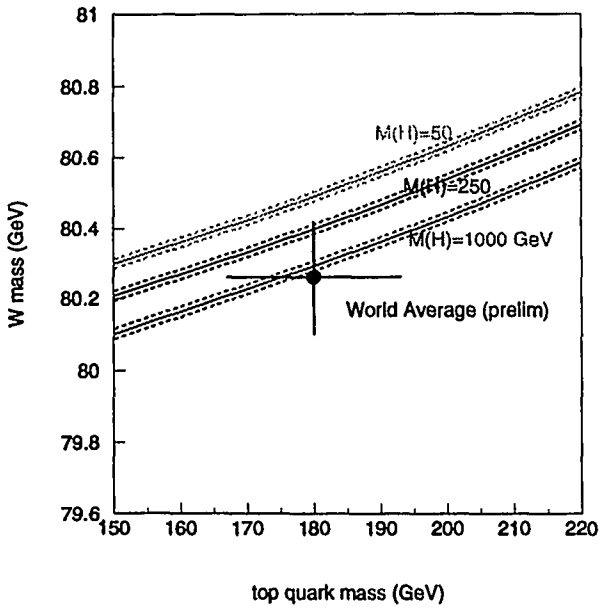

Figure 13: The relationship between M_W and M_{top} in the minimal Standard Model for different values of the Higgs mass. The dotted lines show the variation with the uncertainty on $\alpha_{EM}(M_W)$, which is the dominant uncertainty. The point shows the world averages of the measurements of M_W and M_{top}.

4 Studies of Diboson Final States

An interesting consequence of the non-Abelian gauge symmetry $SU(2)_L \times U(1)_Y$ is that the electroweak gauge bosons should be self-coupling. In particular, the SM predicts nonzero trilinear couplings for $WW\gamma$ and WWZ. It is possible to test these couplings by studying final states involving two bosons: $W\gamma$, $Z\gamma$, WW, WZ, etc. The amplitudes from the s-channel trilinear diagrams usually interfere destructively with amplitudes from other u- and t-channel diagrams, and the diboson production rate is near its minimum for the trilinear coupling strengths dictated by the Standard Model. For models with non-SM coupling values, this cancellation is spoiled, and the coupling constants must be regulated by form factors characterized by a scale Λ_{FF} in order to preserve unitarity.

A formalism has been developed to describe the $WW\gamma$ and WWZ interactions beyond the SM.[30] If Lorentz invariance, C, P, CP invariance, and $U(1)_{EM}$ gauge invariance are assumed, the most general Lagrangian describing the three-boson vertex can be written

$$\mathcal{L}_{WWV}/g_{WWV} = ig_1^V(W_{\mu\nu}^\dagger W^\mu V^\nu - W_\mu^\dagger V_\nu W^{\mu\nu}) + i\kappa_V W_\mu^\dagger W_\nu V^{\mu\nu} + \frac{i\lambda_V}{M_W^2} W_{\lambda\mu}^\dagger W_\nu^\mu V^{\nu\lambda} \quad (2)$$

where $V = \gamma$ or Z. In the SM, $\kappa_\gamma = \kappa_Z = 1$ and $\lambda_\gamma = \lambda_Z = 0$.

4.1 $W\gamma$

The most abundant diboson final state is $W\gamma$. It is studied in both the $e\nu\gamma$ and $\mu\nu\gamma$ channels. The most important selection criteria used by CDF and DØ are shown in Table 3. Note that a minimum photon E_T and a minimum separation between the photon and the lepton, $\Delta R(\ell\gamma) = \sqrt{\Delta\phi(\ell\gamma)^2 + \Delta\eta(\ell\gamma)^2}$, are required. These requirements are necessary even in the theoretical predictions in order to avoid infrared and collinear divergences from photon radiation from the final state leptons.

CDF reports 109 $W\gamma$ events with $E_T^\gamma > 7$ GeV from a preliminary analysis of 67 pb^{-1} of data from Run 1A (Ref. 31) and part of Run 1B. DØ has a final sample 23 events with $E_T^\gamma > 10$ GeV from Run 1A (14 pb^{-1}) (Ref. 32). The photon E_T spectra from these samples is shown in Fig. 14. The main background in these samples is $W + jet$ events in which the jet fakes a photon. Both the normalization and the shape of these spectra are in good agreement with the

Requirement	CDF	DØ
electron acceptance	$\|\eta_e\| < 1.1$	$\|\eta_e\| < 1.1$ or $1.5 < \|\eta_e\| < 2.5$
muon acceptance	$\|\eta_\mu\| < 0.6$	$\|\eta_\mu\| < 1.7$
photon acceptance	$\|\eta_\gamma\| < 1.1$	$\|\eta_\gamma\| < 1.1$ or $1.5 < \|\eta_\gamma\| < 2.5$
photon E_T	$E_T^\gamma > 7$ GeV	$E_T^\gamma > 10$ GeV
γ-ℓ separation	$\Delta R(\ell\gamma) > 0.7$	$\Delta R(\ell\gamma) > 0.7$

Table 3: Selection requirements for $W\gamma$ and $Z\gamma$ events.

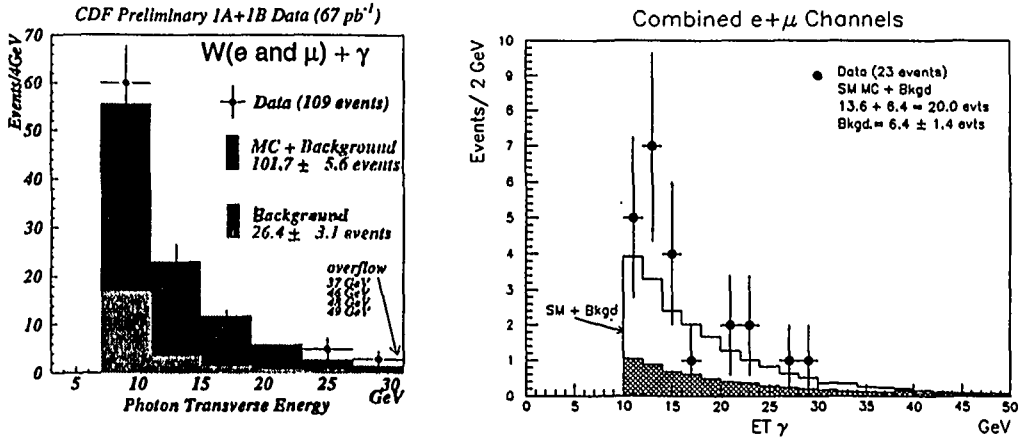

Figure 14: The transverse energy spectra of the photons in the $W\gamma$ samples from (left) preliminary CDF Run 1A plus partial Run 1B (67 pb^{-1}) and (right) DØ Run 1A (14 pb^{-1}).

Standard Model predictions. Both of these facts are significant, since a deviation from SM couplings should result in a higher overall cross section and a harder spectrum for E_T^γ. Limits on $\Delta\kappa$ ($\Delta\kappa = \kappa - 1$) and λ are obtained from fits to these E_T^γ spectra. The 95% CL contours are shown in Fig. 15. The limits on the axes are

$$\text{CDF (prelim.):} \begin{cases} -1.8 < \Delta\kappa < 2.0 & (\lambda = 0) \\ -0.7 < \lambda < 0.6 & (\Delta\kappa = 0); \end{cases}$$

$$\text{DØ:} \begin{cases} -1.6 < \Delta\kappa < 1.8 & (\lambda = 0) \\ -0.6 < \lambda < 0.6 & (\Delta\kappa = 0), \end{cases}$$

where a form factor with $\Lambda_{FF} = 1.5$ TeV has been assumed in both analyses. The magnetic dipole moment ($\mu_W = (\kappa + \lambda + 1)e/2M_W$) and the electric quadrupole moment ($Q_W = -(\kappa - \lambda)e/M_W^2$) of the W boson can be expressed as linear combinations of κ and λ. The lines for $\mu_W = 0$ and $Q_W = 0$ are shown in Fig. 15, and it can be seen that the point where both moments vanish can now be excluded.

A particular SM prediction for $W\gamma$ production is that the destructive interference between the s-channel diagram and the t- and u-channel diagrams should produce a sharp minimum in the angular distribution. This so called "gauge zero"[33] should occur at $\cos(\theta^*) = \pm 0.3$, where θ^* is the angle between the photon and the incoming quark direction in the $W^\mp\gamma$ rest frame. The calculation of θ^* requires one to solve for the unknown longitudinal component of the neutrino momentum, which generally involves a two-fold ambiguity. The cancellation of the amplitudes is destroyed as the couplings deviate from their SM values, so the gauge zero can provide another test for anomalous couplings. The prominence of the zero in the distribution is degraded, however, by the presence of background, by resolution effects, and by contributions from radiative decays. The preliminary distribution of $\cos(\theta^*)$ from CDF is shown in Fig. 16. This sample has had additional requirements placed on it to suppress the contributions from radiative decays, and the $W^+\gamma$ events have been added to the $W^-\gamma$ events after inverting the sign of $\cos(\theta^*)$.

CDF has also investigated some charge asymmetries in $W\gamma$ production using an independent sample of events in which the photons are detected in the region $1.1 < |\eta_\gamma| < 2.4$. In Fig. 17, the first plot shows the rapidity distribution of the photons, signed by the charge of the lepton from the W boson decay. This shows a strong asymmetry, which originates in part from the difference in magnitude of electric charge between *up* and *down* quarks. The forward/backward asymmetry

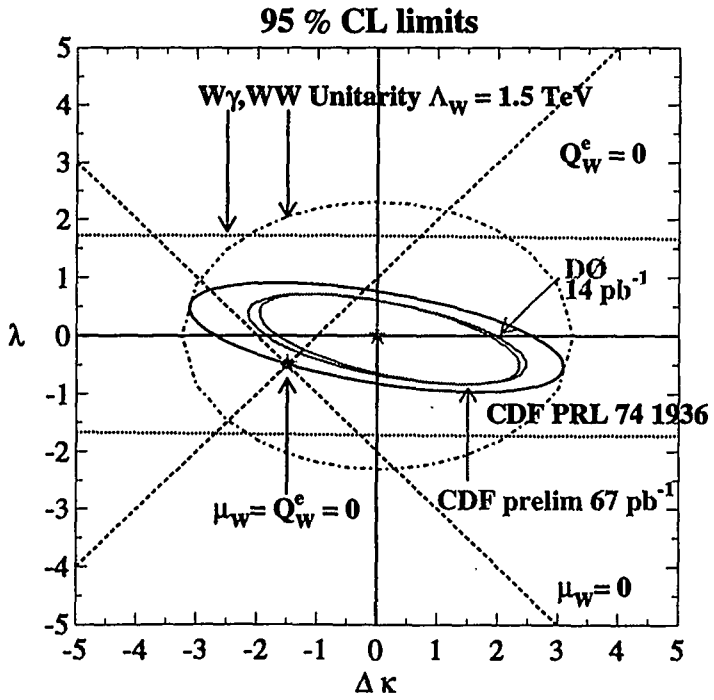

Figure 15: The limits (95% CL) on anomalous coupling parameters λ and $\Delta\kappa$ derived from the $W\gamma$ samples. The dashed lines show the places where the magnetic dipole moment and electric quadrupole moment vanish, and the star indicates the Standard Model prediction. The dot-dashed ellipses show the limits implied by unitarity when a form factor scale of 1.5 TeV is assumed.

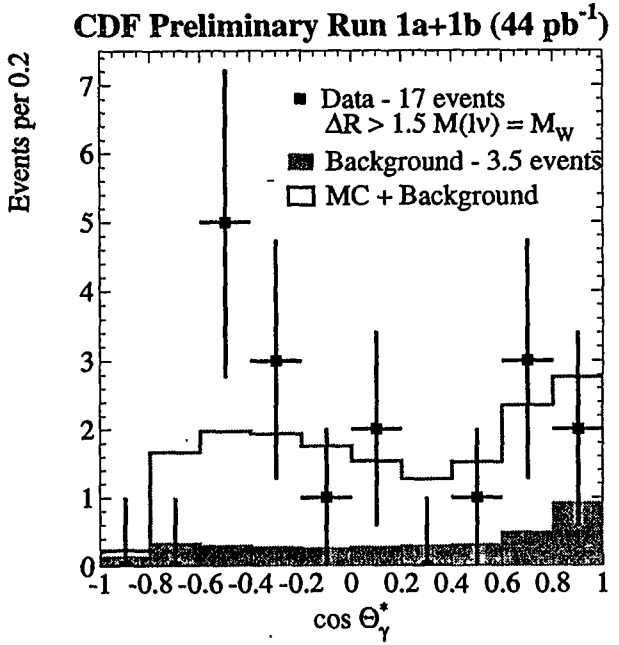

Figure 16: The preliminary CDF data distribution (points) for $\cos\theta^*$ is compared to the expected signal plus background distribution (histogram). The shaded portion of the histogram shows the expected background contribution.

measured on this sample is 0.77 ± 0.07, and it is in good agreement with the prediction of 0.76 ± 0.04. The second figure shows the rapidity difference between the lepton and the photon ($\eta_\gamma - \eta_\ell$), where again the quantity is signed by the lepton charge. The dip in the middle results largely from the requirement that the photons are in the end regions while the leptons are central. The asymmetry measured for the rapidity difference is 0.70 ± 0.04.

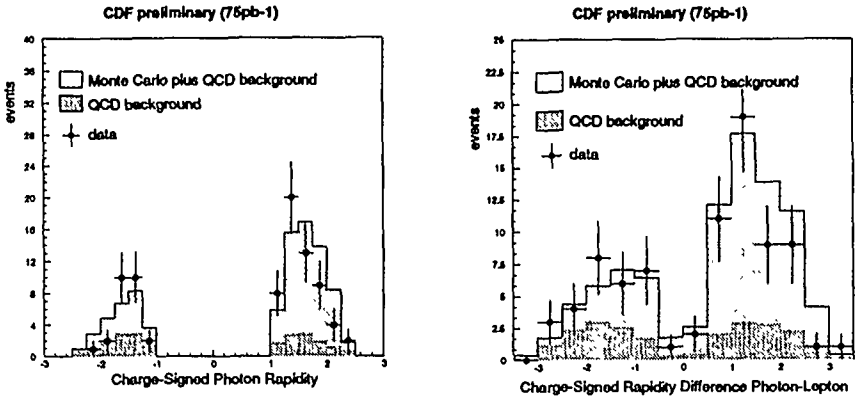

Figure 17: The CDF preliminary distributions of photons in the "plug" region ($1.1 < |\eta| < 2.4$) in $W\gamma$ events. The rapidity is shown on the left, and the rapidity difference $\eta(\gamma) - \eta(\ell)$ of the photon and lepton is shown on the right, and each is signed by the charge of the lepton. The points are the data and the histograms are the predictions for Standard Model plus background.

4.2 $Z\gamma$

The Z boson is a neutral particle, so the SM predicts no direct $Z\gamma$ couplings, although $Z\gamma$ production is still allowed through the t- and u-channels. A more general non-SM formalism,[34] similar to that used for the $W\gamma$, allows for nonzero anomalous couplings given by the parameters h^Z_{10}, h^Z_{20} (CP violating) and h^Z_{30}, h^Z_{40} (CP conserving). The same general features apply: anomalous couplings tend to increase the production cross section and make the photon spectra harder.

Both DØ and CDF have completed preliminary $Z\gamma$ analyses which include Run 1A (Refs. 35, 36) and part of Run 1B. The E^γ_T spectra from these samples is

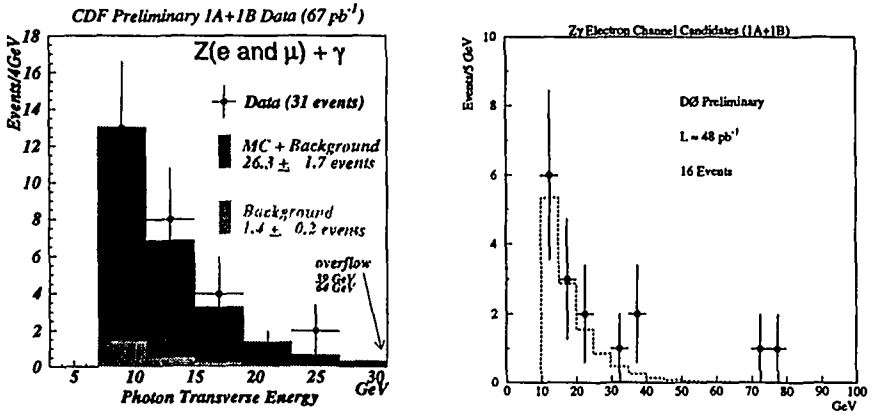

Figure 18: Preliminary distribution of the transverse energy of photons in $Z\gamma$ events from Run 1A plus partial Run 1B from (left) CDF (67 pb^{-1}) and (right) DØ (48 pb^{-1}). The points are the data and the histograms are the expectations of Standard Model plus background.

shown in Fig. 18. The limits on anomalous couplings from CDF are derived from fits to the E^γ_T distribution of the sample shown, while the DØ result is presently only from the Run 1A spectrum (14 pb^{-1}). The limit contours are shown in Fig. 19. The limits on the axes are:

$$\text{CDF (prelim.):} \begin{cases} -1.6 < h^Z_{30}(h^Z_{10}) < 1.6 & (h^Z_{40}(h^Z_{20}) = 0); \\ -0.4 < h^Z_{40}(h^Z_{20}) < 0.4 & (h^Z_{30}(h^Z_{10}) = 0) \end{cases}$$

$$\text{DØ:} \begin{cases} -1.9 < h^Z_{30}(h^Z_{10}) < 1.8 & (h^Z_{40}(h^Z_{20}) = 0) \\ -0.5 < h^Z_{40}(h^Z_{20}) < 0.5 & (h^Z_{30}(h^Z_{10}) = 0), \end{cases}$$

where a form factor with $\Lambda_{FF} = 0.5$ TeV has been assumed.

4.3 WW and WZ

The cleanest channels for detecting pairs of W bosons are those where both bosons decay leptonically. The signatures are then $ee+\not{p}_T$, $e\mu+\not{p}_T$, and $\mu\mu+\not{p}_T$, where the $\not{p}_T$ comes from the vector sum of the two neutrino momenta. DØ has searched for WW production in these modes in Run 1A (Ref. 37) (14 pb^{-1}), and CDF has a preliminary result based on Run 1A and part of Run 1B (67 pb^{-1}). DØ

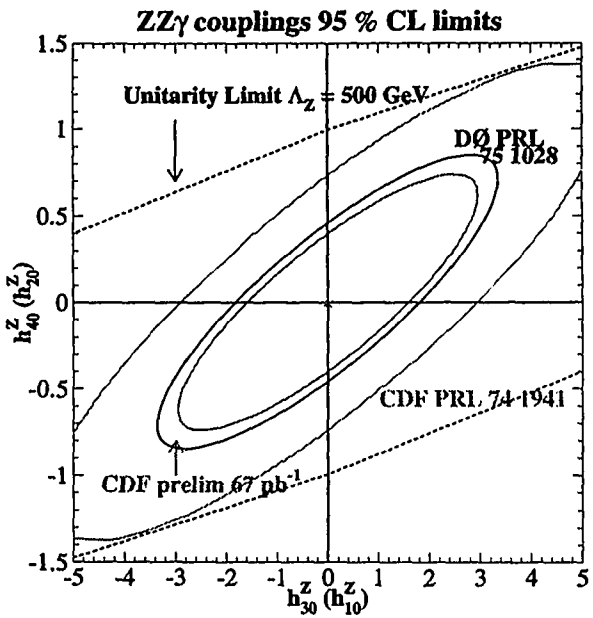

Figure 19: The limits (95% CL) on anomalous coupling parameters $h^Z_{10}, h^Z_{20}, h^Z_{30}, h^Z_{40}$ derived from the $Z\gamma$ samples. The Standard Model prediction is at the center (0,0). The dotted ellipses show the limits implied by unitarity when a form factor scale of 0.5 TeV is assumed.

observes one event, with an expected background of 0.56±0.13 events and expected SM signal of 0.47 ± 0.07 events. CDF observes five events, with expectations of 1.23 ± 0.43 events background and 2.6 ± 0.9 events signal. From these samples, DØ calculates an upper limit (95% CL) of 87 pb on the cross section for WW production. CDF calculates a cross section of $13.8 \pm^{9.2}_{7.4} \pm 2.9$ pb. DØ also quotes limits on anomalous coupling from this analysis, with the assumption that $\kappa^\gamma = \kappa^Z$ and $\lambda^\gamma = \lambda^Z$:

$$\text{DØ:} \begin{cases} -2.6 < \Delta\kappa < 2.8 & (\lambda = 0) \\ -2.1 < \lambda < 2.1 & (\Delta\kappa = 0). \end{cases}$$

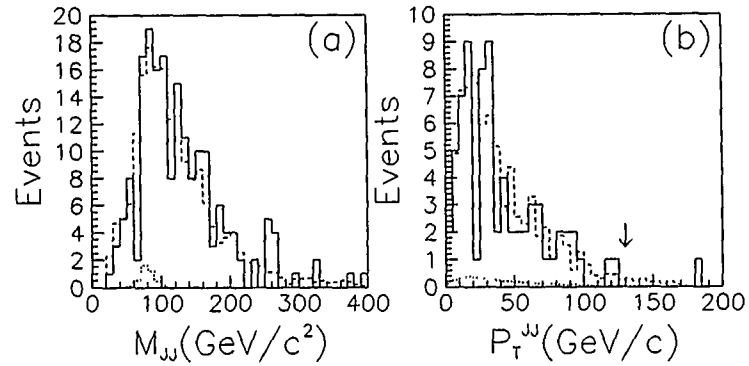

Figure 20: The sample selection for the CDF $WW \to \ell\nu jj$ analysis. The invariant mass spectrum of the two jets is shown in (a) prior to any cut on $M(jj)$. The $p_T(jj)$ spectrum after the cut of $60 < M(jj) < 110$ GeV is shown in (b). The arrow indicates the final cut of $p_T(jj) > 130$. The solid histograms are the data, the dashed histograms are the expected background, and the dotted histograms are the expectations from SM diboson production.

The small rates in the pure leptonic channels of WW decay make it attractive to consider the case where one W boson decays hadronically to two jets. The signature is then $\ell jj + \not{p}_T$. In this case, the experiments do not distinguish $W \to jj$ from $Z \to jj$, so it is the sum of WW and WZ which contributes to signal. The largest background is from production of single W bosons accompanied by two

jets. This background is reduced by both CDF and DØ by requiring that the jj invariant mass be consistent with that of a W or Z boson. Figure 20 shows the jj mass spectrum from CDF[38] before the requirement $60 < M_{jj} < 110$ GeV was imposed, and the p_T^{jj} spectrum afterwards. Even after the M_{jj} requirement, the sample is dominated by single W plus two-jet events. Since the high p_T portion of the spectrum is greatly enhanced by anomalous couplings, CDF requires $p_T^{jj} >$ 130 GeV, after which one event remains. The preliminary DØ analysis is similar, except that no cut is made on p_T^{jj}, and instead, a fit is made to the $p_T^{e\nu}$ spectrum (shown in Fig. 21) from which the anomalous coupling limits are derived. With the same assumption of the equality of λ and κ for photons and Z bosons, the limits obtained from the $\ell\nu jj$ analyses are:

$$\text{CDF:} \begin{cases} -1.11 < \Delta\kappa < 1.27 & (\lambda = 0) \\ -0.81 < \lambda < 0.84 & (\Delta\kappa = 0); \end{cases}$$

$$\text{DØ (prelim.):} \begin{cases} -0.89 < \Delta\kappa < 1.07 & (\lambda = 0) \\ -0.66 < \lambda < 0.67 & (\Delta\kappa = 0), \end{cases}$$

where a form factor with $\Lambda_{FF} = 1$ TeV is used by CDF and $\Lambda_{FF} = 1.5$ TeV is used by DØ.

5 Conclusion

Recent analyses of W and Z boson events from the Fermilab Tevatron Collider have resulted in a considerable improvement in the measurements of the properties of the W boson. The W mass is now measured to about 0.2%, while the W width is measured to about 15% (3%) directly (indirectly). The best limit on the anomalous coupling parameters $\Delta\kappa$ and λ are around 1.1 and 0.6, respectively. The anomalous couplings of the Z bosons have also been tested.

In most cases, these results were obtained from only a fraction of the data that will be available from the complete Run 1 of the Tevatron Collider. A total sample of about 100 pb^{-1} is expected for each experiment. When these data are analyzed (within the next year, probably), the precision of the electroweak measurements should be considerably improved. The uncertainty on the W mass, for example, should be reduced to around 80 MeV. The next major improvement is then expected in Run 2 of the Tevatron Collider, which is scheduled to begin in 1999 and to provide samples of about 2000 pb^{-1} for the upgraded versions of CDF and DØ.

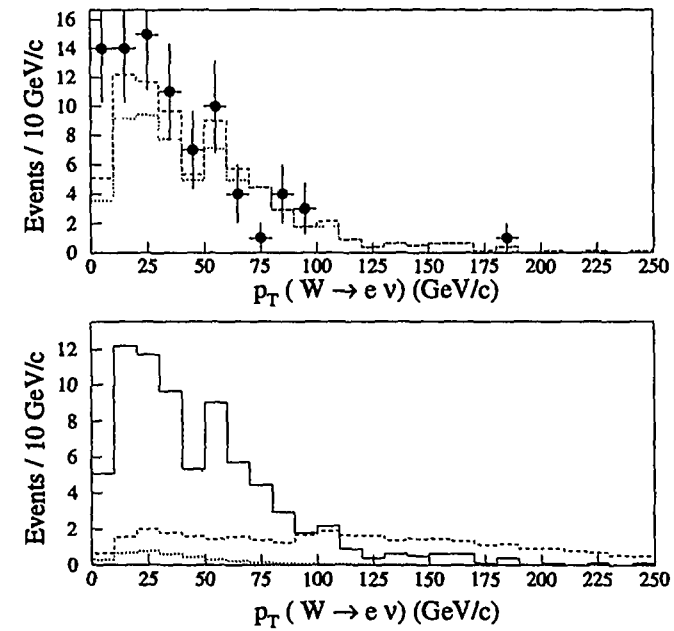

Figure 21: The preliminary DØ $p_T(e\nu)$ distributions for $WW \to e\nu jj$. The upper figure shows the data (points) compared to the expected background (dashed histogram). The lower figure shows the expected background (solid histogram) compared to predictions for SM WW production (dotted) and as an example ($\Delta\kappa = 2, \lambda = 1.5$) of anomalous couplings (dashed).

References

[1] G. Arnison *et al.* (UA1 Collaboration), Phys. Lett. B **122**, 103 (1983); G. Arnison *et al.* (UA1 Collaboration), Phys. Lett. B **129**, 273 (1983).

[2] M. Banner *et al.* (UA2 Collaboration), Phys. Lett. B **122**, 476 (1983); P. Bagnaia *et al.* (UA2 Collaboration), Phys. Lett. B **129**, 130 (1983).

[3] F. Abe *et al.* (CDF Collaboration), Nucl. Instrum. Methods A **271**, 387 (1988).

[4] S. Abachi *et al.* (DØ Collaboration), Nucl. Instrum. Methods A **338**, 185 (1994).

[5] S. Abachi *et al.* (DØ Collaboration), Phys. Rev. Lett. **75**, 1456 (1995).

[6] F. Abe *et al.* (CDF Collaboration), Phys. Rev. Lett. **64**, 152 (1990); F. Abe *et al.* (CDF Collaboration), Phys. Rev. D **44**, 29 (1991); F. Abe *et al.* (CDF Collaboration), Phys. Rev. Lett. **69**, 28 (1992).

[7] F. Abe *et al.* (CDF Collaboration), Phys. Rev. Lett. **73**, 220 (1994); F. Abe *et al.* (CDF Collaboration), Phys. Rev. D **52**, 2624 (1995); W. F. Badgett in *Proceedings of the 8th DPF Meeting*, August 2-6 (1994), 431 (Albuquerque, New Mexico).

[8] C. Albajar *et al.* (UA1 Collaboration), Phys. Lett. B **253**, 503 (1991).

[9] J. Alitti *et al.* (UA2 Collaboration), Phys. Lett. B **276**, 365 (1992).

[10] R. Hamberg, W. L. van Neerven, and T. Matsuura, Nucl. Phys. B **359**, 343 (1991); W. L. van Neerven and E. B. Zijlstra, Nucl. Phys. **382**, 11 (1992).

[11] Particle Data Group, L. Montanet *et al.*, Phys. Rev. D **50**, 1173 (1994).

[12] J. L. Rosner, M. P. Worah, and T. Takeuchi, Phys. Rev. D **49**, 1363 (1994).

[13] F. Abe *et al.* (CDF Collaboration), Phys. Rev. Lett. **74**, 341 (1995).

[14] F. Abe *et al.* (CDF Collaboration), Phys. Rev. Lett. **74**, 850 (1995).

[15] W. Giele, E. Glover, and D. A. Kosower, Nucl. Phys. B **403**, 663 (1993).

[16] M. Glück, E. Reya, and A. Vogt, Z. Phys. C **67**, 433 (1995); S. Kretzer, E. Reya, and M. Stratmann, DO-TH 94/26, December 1994.

[17] H. L. Lai *et al.*, Phys. Rev. D **51**, 4763 (1995).

[18] A. D. Martin, R. G. Roberts, and W. J. Stirling, Phys. Rev. D **50**, 6734 (1994).

[19] P. de Barbaro in *Proceedings of the 10th Topical Workshop on Proton-Antiproton Collider Physics*, Batavia, Illinois, 9-13 May, 1995.

[20] F. Abe *et al.* (CDF Collaboration), Phys. Rev. Lett. **75**, 11 (1995); F. Abe *et al.* (CDF Collaboration), Phys. Rev. D **52**, 4784 (1995).

[21] J. Alitti *et al.* (UA2 Collaboration), Phys. Lett. B **276**, 354 (1992).

[22] F. Abe *et al.* (CDF Collaboration), Phys. Rev. Lett. **65**, 2243 (1990); F. Abe *et al.* (CDF Collaboration), Phys. Rev. D **43**, 2070 (1991); the 88/89 cross sections should be increased by 1/0.907 for consistent comparison with the Run 1 cross sections.

[23] S. Rajagopalan in *Proceedings of Les Rencontres de Physique de la Vallee d'Aoste*, La Thuile, Italy, 5-11 March, 1995.

[24] The LEP Electroweak Working Group, CERN Report No. CERN/PPE/94-187 (1994), unpublished.

[25] K. Abe *et al.* (SLD Collaboration), Phys. Rev. Lett. **73**, 25 (1994).

[26] C. Arroyo *et al.* (CCFR Collaboration), Phys. Rev. Lett. **72**, 3452 (1994).

[27] F. Halzen and B. A. Kniehl, Nucl. Phys. B **353**, 567 (1991).

[28] F. Abe *et al.* (CDF Collaboration), Phys. Rev. Lett. **74**, 2626 (1995).

[29] S. Abachi *et al.* (DØ Collaboration), Phys. Rev. Lett. **74**, 2632 (1995).

[30] K. Hagiwara, R. D. Peccei, D. Zeppenfeld, and K. Hikasa, Nucl. Phys. B **274**, 253 (1987); U. Baur and D. Zeppenfeld, Phys. Lett. B **201**, 383 (1988).

[31] F. Abe *et al.* (CDF Collaboration), Phys. Rev. Lett. **74**, 1936 (1995).

[32] S. Abachi *et al.* (DØ Collaboration), Phys. Rev. Lett. **75**, 1034 (1995).

[33] K. O. Mikaelian, Phys. Rev. D **17**, 750 (1978); K. O. Mikaelian, M. A. Samuel, and D. Sahdev, Phys. Rev. Lett. **43**, 746 (1979); R. W. Brown, K. O. Mikaelian, and D. Sahdev, Phys. Rev. D **20**, 1164 (1979); T. R. Grose and K. O. Mikaelian, Phys. Rev. D **23**, 123 (1981); S. J. Brodsky and R. W. Brown, Phys. Rev. Lett. **49**, 966 (1982); M. A. Samuel, Phys. Rev. D **27**, 2724 (1983); R. W. Brown, K. L. Kowalski, and S. J. Brodsky, Phys. Rev. D **28**, 624 (1983); R. W. Brown and K. L. Kowalski, Phys. Rev. D **29**, 2100 (1984).

[34] K. Hagiwara *et al.*, Nucl. Phys. B **282**, 253 (1987).

[35] F. Abe *et al.* (CDF Collaboration), Phys. Rev. Lett. **74**, 1941 (1995).

[36] S. Abachi *et al.* (DØ Collaboration), Phys. Rev. Lett. **75**, 1028 (1995).

[37] S. Abachi *et al.* (DØ Collaboration), Phys. Rev. Lett. **75**, 1023 (1995).

[38] F. Abe *et al.* (CDF Collaboration), Phys. Rev. Lett. **75**, 1017 (1995).